Plant-based Corrosion Inhibitor from Extracts of *Cerbera Odollam*: Study of Inhibition Efficiency on Mild Steel in Various Electrolyte Conditions

Nur Adryna binti Mohd Rosli and Nor Roslina Rosli

Faculty of Chemical Engineering, Universiti Teknologi MARA

***Abstract*—Extracts of oil from sea mango (*Cerbera Odollam)* seeds was investigated in terms of its corrosion inhibition potentials via weight loss measurements and potentiodynamic Tafel polarization technique. It was found that sea mango oil reduced corrosion rate and increased inhibition efficiency as inhibitor concentration and pH test solution increased from 2 to 7. Structural characterization of active corrosion compounds in oil samples was analysed using FT-IR and GCMS. Phytochemical screening tests were performed to detect the presence of saponin, phenol, steroid and tannin. The inhibitive properties of these extracts were likely due to the presence of oxygen and nitrogen atoms, which have evidenced from FTIR and GCMS. The adsorption of sea mango oil was found to best fit Langmuir adsorption isotherm.**

Keywords— Sea mango oil. Tafel plots, weight loss test, organic corrosion inhibitor.

I. INTRODUCTION

Mild steel, also known as carbon steel has become a stealing praise for its versatility and cost effectiveness, which most can deliver good performances for many applications [1]. Despite the glorious side, mild steels prone to have week corrosion resistance. Industrial processes such as acid cleaning, pickling, and descaling utilizes extensive acid-bearing fluids that results in exposing metal surfaces to corrosion [2]. Previously, researchers have made studies on cathodic protection and the use of corrosion inhibitor on steel. Among these two methods, the use of corrosion inhibitor is more economical, practical and convenient compared to cathodic protection [3]. However, the application of synthetic organic corrosion inhibitors is at stake where toxicity, time and cost of manufacturing are in doubt. On the other hand, inorganic inhibitors, particularly those which contain phosphate, chromate and heavy metals have been given negative feedback by marine industry where aquatic life is at stake [4]. Today, researchers have shifted their interests on natural inhibitors extracted from plants due to adequate effects as corrosion inhibitors that can mimic inhibitors in industry [5] and green corrosion inhibitors are easily decomposed and free from toxic materials [6].

II. METHODOLOGY

A. Materials

Sea mango oil was extracted from seed or kernel of the mature fruit of *Cerbera Odollam.* The fruits were collected around Morib Beach, Malaysia (2°44'55.5"N 101°26'36.5"E). The oil was extracted using methanol as solvent, via Soxhlet extraction. The percentage oil yield for every temperature used was studied.

B. FTIR (Fourier Transform Infrared Spectrometry)

The components of *Cerbera Odollam* seeds oil was investigated to determine the functional groups present in the compound. The *Cerbera Odollam* seeds was examined using FT-IR Spectrum One Perkin Elmer model with the wavelength range of 515- 4000 cm^{-1}. Potassium bromate (KBr) was used as background material in the analysis.

C. GC-MS (Gas Chromatography Mass Spectrometry)

Organic components present in the *Cerbera Odollam* seeds were investigated in a Varian 3800 GC Gas Saturn 2000 GC-MS. The gas chromatography column was equipped with capillary column (15 m × 0.53 mm, 0.5 µm film) and Flame Ionization Detector (FID) as detector. Nitrogen gas was used as carrier gas in GCMS. The initial temperature of oven was set at 120 °C for 5 minutes before raising it to 260 °C for 8 minutes at the rate of 20 °C/minute. Aside from that, the temperature of detector and injector were set at 260 °C and 230 °C respectively.

D. Formulation of Corrosion Inhibitor

The sea mango oil must be firmly soluble in solution for it to be used as corrosion inhibitor. *Cerbera Odollam* seeds oil obtained from solvent extraction was inherently insoluble in test solution within range of working pH and concentration. Emulsifier, poly(oxyethelene)x-sorbitane-monolaurate or commercially known as Tween 20 (T20) was used to make it soluble. Ratio of 5:0.5, 5:1.0 and 5:1.5 were studied in immersion test before selecting the best formulation of inhibitor to T20.

E. Preparation of Mild Steel Specimens

Mild steel grade AISI 1018 was used. Rectangular specimens of size 2 cm x 2 cm x 0.6 cm were used for weight loss experiment and Potentiodynamic Tafel Polarization. As for pre-treatment prior to the experiment, the mild steels specimens were polished with emery papers (grade 400, 600 and 800). Then, specimens were cleaned with distilled water followed by degreasing with acetone and finally dried.

F. Potentiodynamic Tafel Polarization

Tafel polarization was carried out using electrochemical work station (Metrohm Autolab Potentiostat) connected to electrochemical in a Pyrex glass cell with a tree-electrode, platinum, Ag/AgCl and mild steel AISI 1018 as counter electrode, reference electrode and working electrode, respectively. Polished

mild steel specimens of 4 cm² exposal area were immersed in 100 ml test solution with absence and presence corrosion inhibitor at different concentrations from pH 2, pH 5 and pH 7. Samples were prepared as shown in Figure 1.

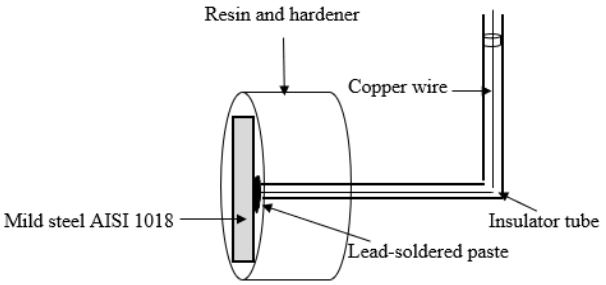

Fig. 1: Sample assembly for Potentiodynamic Tafel Polarization

This experiment was using OCP range of -250 mV to +250 mV with sweep rate of 80 mV/min. Sweep rate that being set determined the linearity of Tafel polarization curve [7]. Cathodic portion and anodic portion of the Tafel were scanned from 250 mV to 0 and 0 to +250 mV, respectively. By extrapolating the linear segments of anodic and cathodic polarization curves to corrosion potential (Ecorr) at different concentration of formulated corrosion inhibitor, corrosion density (Icorr) was obtained [8].The inhibition efficiency was calculated using:

$$IE(\%) = \frac{I_{corrblank} - I_{corri}}{I_{corrblank}} \; x \; 100\%$$

Where $I_{corrblank}$ is corrosion current density without corrosion inhibitor and I_{corr} is corrosion current density with inhibitor at different concentrations.

G. *Weight Loss Test*

Mild steel specimens size 2 cm × 2 cm × 0.6 cm were used in weight loss experiments, all in the same manners. After pre-treatment, the specimens were weighted accurately using digital weighing balance, before the specimens were immersed in 200 ml test solutions. This was done in a closed system where the container was covered to prevent any loss of test solutions. The measurements were performed at room temperature of 25 °C for a duration of 5 hours [11]. All the tests were conducted in closed container of solution ratio formulated in pH 2 to 7.

After 5 hours of elapsed time, the specimens were taken out for washing with Clarke's solution and drying process before final weight is measured. The efficiency of corrosion inhibitor (IE%) was determined by using the following equation:

$$IE\% = \frac{Wo - Wi}{Wo} \times 100$$

where Wi and W_O are the weight loss value in presence and absence of inhibitor, respectively. The corrosion rate (CR) in mm/year of mild steels was determined using the following equation:

$$c_R = \frac{87.6W}{AtD}$$

where W is the weight loss of mild steel (mg), A was the area of specimen (cm^2), t is the immersion time (hr), and D is the density of mild steel (g/cm^3).

III. RESULTS AND DISCUSSION

A. *The effects of temperature on oil extract yield via Soxhlet Apparatus.*

The oil yield percentage increased with increase in temperature, which was highest at 150°C as shown in Figure 2. This was probably due to the increase of solubility and diffusivity of solvent onto the samples, which then improved the mass transfer. The solvent used in the extraction, which was methanol, was a polar solvent.

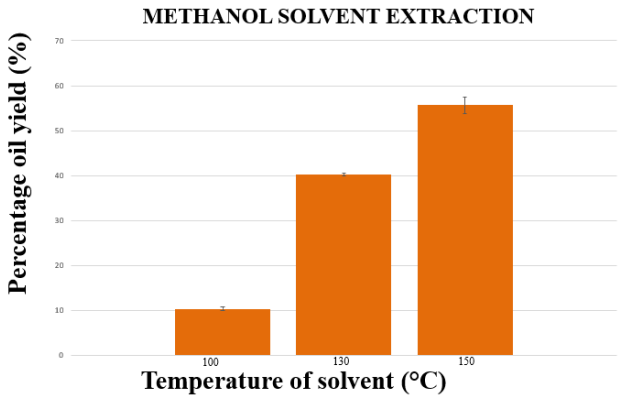

Fig. 1: Effect of temperature on extracted oil yield percentage.

B. *Phytochemical Screening Test*

Phytochemical test results were summarized as in Table 2. Tests were conducted to detect the presence of saponins, phenols, steroids, and tannins. Among all tests conducted, only steroids showed positive result.

Table 1: Phytochemical Tests

Phytochemical Tests	Observation	Appendix	Conclusion
Saponin Test	No warm froth formed		Saponin absent
Phenol Test	No green precipitate formed		Phenol absent
Steroid Test	Reddish to brownish layer formed at interface		Steroid presence
Tannin Test	No blue or green precipitate formed in the filtrate	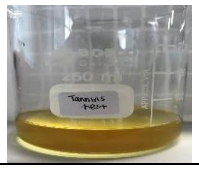	Tannin absent

C. *Characterization of Sea Mango oil using FTIR*

The FTIR spectra for sea mango oil is shown in Figure 3. A medium broad adsorption peak around 3281 cm^{-1} displayed the presence of O-H stretch. This could be presented by alcohol, phenol or/and carboxylic acid compound. The weak peak at 2119 cm^{-1} indicated the presence of alkenyl C≡C stretch. The observed weak-medium peak of 1640 cm^{-1} depicted the presence of N-H bending in the sea mango oil. On the other hand, few weak adsorption peaks around 1413 cm^{-1} to 1457 cm^{-1} portrayed the existence of alkenyl C=C stretches. The last two absorption peaks represented C-O which dedicated to the presence of ester due to the more than one weak stretches. This anticipated the existence of functional groups that contain heteroatoms such as oxygen and nitrogen which were active ingredients as inhibitor.

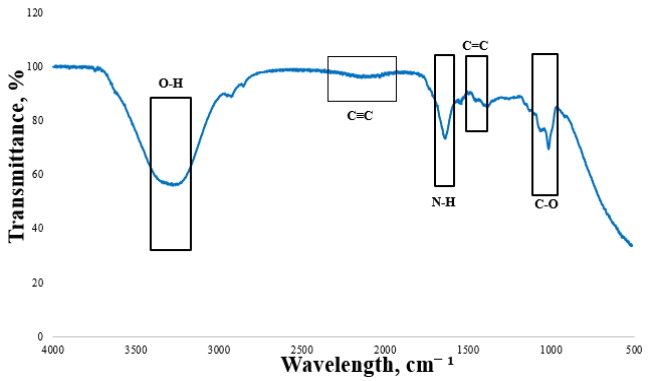

Fig. 3: Fourier Transform Infra-Red (FTIR) Spectra for Sea Mango Oil

D. Characterization of Sea Mango Oil by GCMS

Figure 4 shows components detected from GCMS. The main components of sea mango oil were 38.91% silane, trimethyl(nonyloxy) ($C_{12}H_{28}OSi$), 19.85% oleic acid (C18H34O2) and 16.01% tetradecanoic acid (C14H28O2). The minor components were glutamyllysine, 11-Hexadecyn-1-ol, 4,8-Dimethylnona-3,7-dien-2-one, Isopropyl Palmitate and palmitic acid. All components exhibit good inhibitive effects on mild steel due to oxygen and nitrogen atom presence in molecular structures.

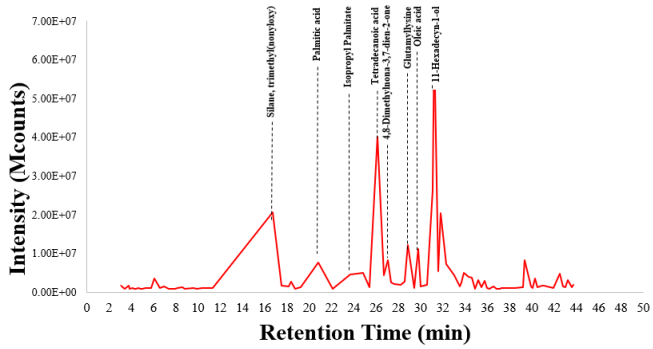

Fig. 4: Gas Chromatography Mass Spectrometry (GCMS) of Sea Mango Oil

E. Optimum Inhibitor Formulation Test.

The maximum ratio of corrosion inhibitor (CI) to emulsifier (T20) was analyzed. In this test, corrosion rate of mild steel AISI 1018 was immersed in 1 M HCl solution comprising different weight ratios of CI to T20 which were 5:0.5, 5:1.0 and 5:1.5 for 4 hours and 24 hours. From Figure 5, 4 hours of immersion resulted in rising of corrosion rate from ratio 5:0.5 to 5:1.0 which were 1.39 mm/year and 1.89 mm/year, respectively. A further increased of time to 24 hours showed similar corrosion rate trend for both 5:0.5 and 5:1.0. However, within this duration, ratio 5:1.5 depicted the highest corrosion rate of 1.29 mm/year. The result showed the solution with weight ratio of 5:05 showed the lowest corrosion rate of both 4 hours and 24 hours. The corrosion rates were calculated from weight loss of the steel specimens.

The weight ratio of 5:0.5 might has reached its critical micelle concentration (CMC). Any increment of T20 might not help to reduce the interface tension (IFT) between 1 M HCl solution and sea mango oil corrosion inhibitor. Further addition of T20 would be added to the micelles. Increase of emulsifier up from this point will not reduce the corrosion rate any lower [9]. Hence, for corrosion test via potentiodynamic Tafel polarization method and weight loss method were using weight ratio CI:T20 of 5:0.5.

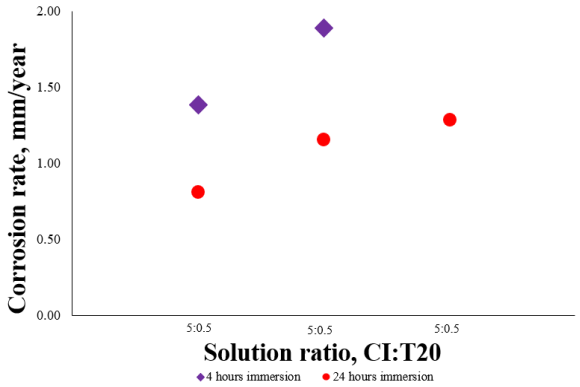

Fig. 5: Corrosion rate of mild steel AISI 1018 immersed in 1 M HCl with weight ratio of 5:0.5, 5:1.0 and 5:1.5

F. Potentiodynamic Tafel Polarization

Figure 6 shows similar trend for all pH that increased of concentration of corrosion inhibitor decrease the corrosion rate of mild steel. This was due to the increase of active ingredients such as oxygen and nitrogen on the surface of mild steel [10]. On top of that, the corrosion rate of mild steel decreases as the pH values increases from pH 2, pH 5, followed by pH 7. Corrosion rate at pH 2 is seen to be the highest in mm/year due to the highest concentration of hydrogen ion (H^+) which participated in the corrosion reaction, compared to pH 5 and pH 7.

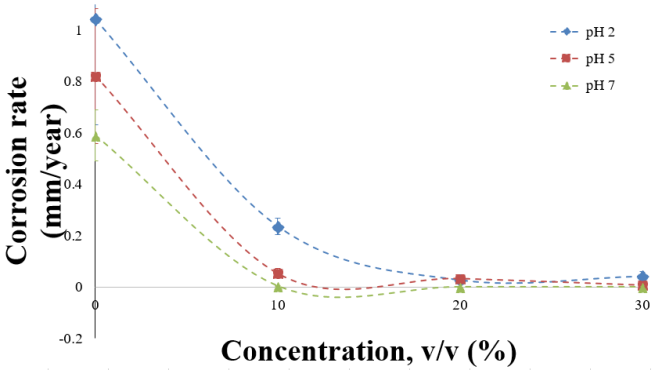

Fig. 6: Corrosion rate of mild steel AISI 1018 in test solutions of pH 2, pH 5 and pH 7 in corrosion inhibitor at various concentrations via electrochemical test.

Figure 7 shows inhibition efficiency of corrosion inhibitor sea mango oil at different concentrations towards mild steel immersed in three different pH values solution. The increase in pH values results in increasing the IE. The general trend observed is that the IE increase with concentration. The similar trend of corrosion rate and IE were observed in weight loss test.

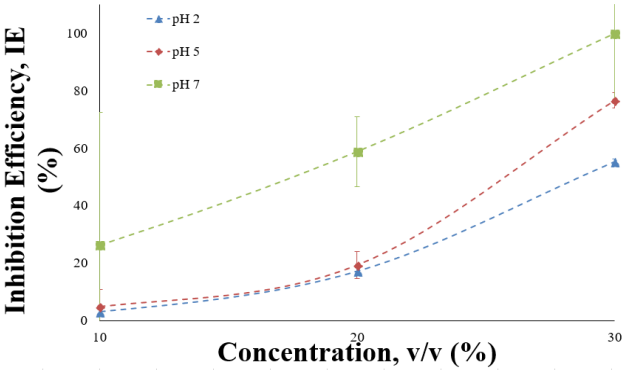

Fig. 7: Inhibition efficiency of mild steel AISI 1018 in test solutions of pH 2, pH 5 and pH 7 in the absence and presence corrosion inhibitor at various concentrations.

Figure 8 (a), (b) and (c) show Potentiodynamic Tafel polarization curve for pH 2, pH 5 and pH 7, respectively in blank solution to solutions of various inhibitor concentrations. It is observed that for blank solution at pH 2, pH 5 and pH 7, cathodic Tafel slopes were higher than anodic Tafel slopes. However, when inhibitor was added to these test solutions, the cathodic Tafel slope of every pH test solutions was reduced. This demonstrates that adsorbed film formed by corrosion inhibitor onto the mild steel reduced the metal oxidation rate [7]. Thus, metal dissolution was reduced.

On top of that, Figure 6 also portrays clear shift in both anodic and cathodic Tafel slops towards reduction of current density with addition of sea mango oil inhibitor from 10% to 30%. Figure 7 illustrates that current density shifted towards zero value as the pH of test solution increased. As seen, both pH 2 and pH 5 show current density around 0.001 A to near 0.0001 A, meanwhile at pH 7, current density dropped to below 0.0001 A. This is subjected to reduction of corrosion rate from pH 2 to pH 7 which expressed by reduction of electrons released in the test solutions. This is too can be observed from Table 2 that I_{corr} current decreased as inhibitor concentration increased.

pH	C, v/v (%)	Ecorr	ba (mV/dec)	bc (mV/dec)	Icorr	IE (%)
2	0	-427.6	323.7	43.3	0.15942	-
	10	-454.8	96.9	44.9	0.15455	3.1
	20	-462.4	59.9	38.8	0.13212	17.1
	30	-460.8	57.9	38.1	0.07124	55.3
pH	**C, v/v (%)**	**Ecorr**	**ba (mV/dec)**	**bc (mV/dec)**	**Icorr**	**IE (%)**
5	0	-450.1	301.3	63.9	0.01452	-
	10	-444.5	96.9	44.9	0.01381	4.8
	20	-462.4	59.9	38.8	0.01171	19.3
	30	-454.6	79.4	67.3	0.00339	76.7
pH	**C, v/v (%)**	**Ecorr**	**ba (mV/dec)**	**bc (mV/dec)**	**Icorr**	**IE (%)**
7	0	-497.6	150.0	103.4	0.00465	-
	10	-487.6	121.6	121.7	0.00343	26.2
	20	-518.4	171.5	81.1	0.00192	58.8
	30	-501.5	56.4	44.8	2.5E-06	99.9

Table 2: Tafel Parameter from Various Inhibitor Concentrations in Test Solutions of pH 2, pH 5 and pH 7

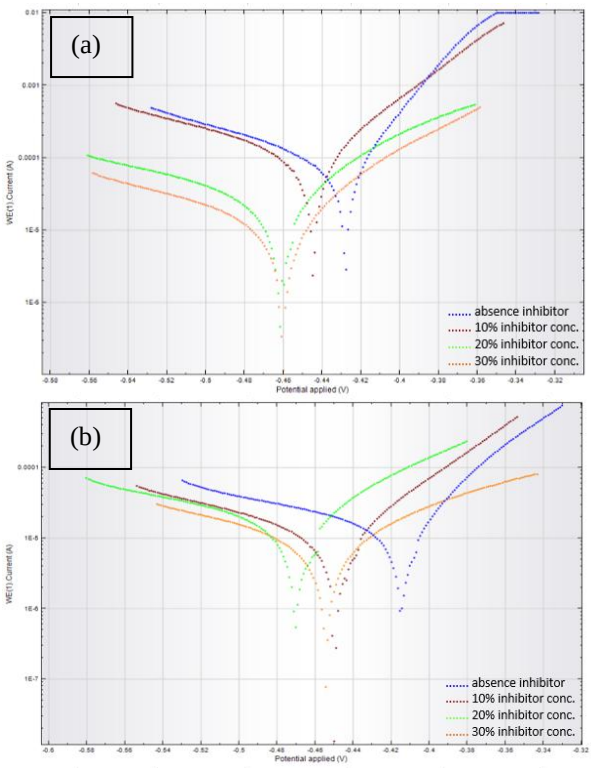

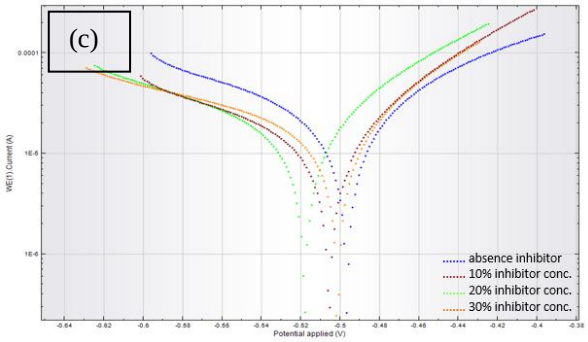

Figure 8: Potentiodynamic Tafel Polarization plots for inhibitor of various concentrations at (a) pH 2, (b) pH 5 and (c) pH 7

G. Weight loss Test

Table 3(a) depicts corrosion rate of AISI 1018 mild steel specimens immersed for 5 hours in test solution of pH 2 to pH 7, with absence and presence of corrosion inhibitor in various concentrations. Figure 9 showed that addition in formulated corrosion inhibitor in water (CIT20H) resulted in decrease of the corrosion rate of mild steel. On top of that, it was observed that corrosion rate decreased with increase of pH. The figure showed highest corrosion rate at pH 2 and the lowest at pH 7.

Table 3(b) portrayed corrosion inhibition efficiency of the samples calculated from weight loss data. The values plotted in Figure 4.7 showed corrosion inhibition (IE) increased with increase of CIT20H, from blank to 30% concentration. This was similar to the trends observed in all pH values. By comparing of all pH of test solutions, pH 2 illustrated the lowest inhibition efficiency followed by other pH values.

CIT20H, v/v (%)	blank	10	20	30
1M HCl, v/v (%)	100	90	80	70
pH values	Corrosion rate (mm/year)			
pH 2	2.621	1.473	1.064	0.632
pH 3	2.206	1.070	0.633	0.206
pH 4	1.995	1.011	0.598	0.195
pH 5	1.578	0.815	0.218	0.206
pH 6	1.245	0.656	0.208	0.196
pH 7	1.010	0.218	0.000	0.000

(a)

CIT20H, v/v (%)	blank	10	20	30
1M HCl, v/v (%)	100	90	80	70
pH values	Corrosion Inhibition (%)			
pH 2	0.000	44.444	57.778	75.556
pH 3	0.000	52.778	72.222	88.889
pH 4	0.000	36.111	63.889	83.333
pH 5	0.000	44.444	72.222	83.333
pH 6	0.000	50.000	83.333	83.333
pH 7	0.000	50.000	100.000	100.000

(b)

Table 3: (a) Corrosion of mild steel AISI 1018 in test solution of pH 2 to 7 (b) inhibition efficiency of mild steel AISI 1018 in test solution of pH 2 to 7, both in absence and presence of corrosion inhibitor at various concentrations

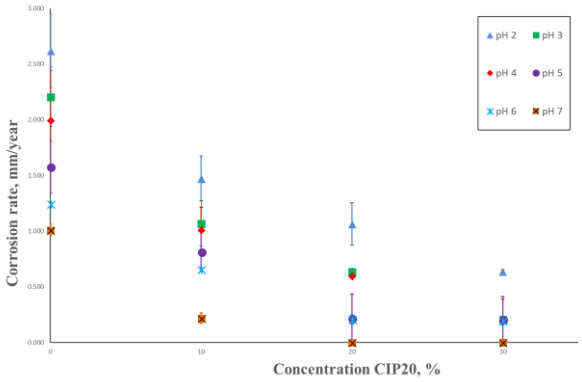

Fig. 9: Corrosion rate from weight loss test of AISI 1018 mild steel specimens immersed in test solutions of pH 2 to 7 with absence and presence of corrosion inhibitor at various concentrations

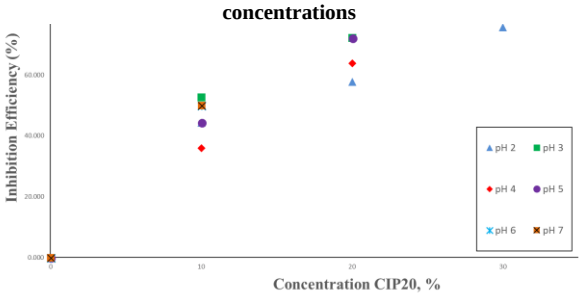

Fig.10: Inhibition efficiency from weight loss test of AISI 1018 mild steel specimens immersed in test solutions of pH 2 to 7 with absence and presence of corrosion inhibitor at various concentrations.

Figure 11 showed isotherm performed by Langmuir isotherm at corrosion inhibitor concentration of 10%, 20% and 30% in test solution of pH 2 to pH 7.

It could be seen from Table 4.6-1, average value of R^2 of Langmuir isotherm was nearer to value 1 which had the lowest residual compared to other isotherms. Hence, Langmuir isotherm was chosen to represent corrosion inhibitor extracted from sea mango oil.

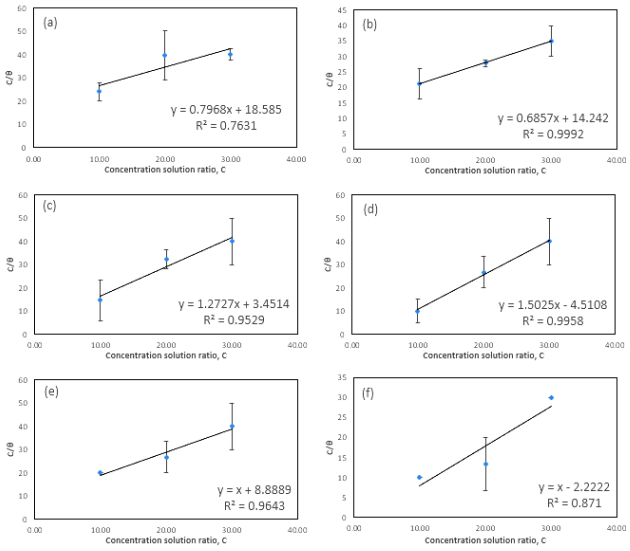

Fig. 11: Langmuir isotherm for adsorption of CIT20H in test solutions of pH (a)2 (b)3 (c)4 (d)5 (e)6 and (f)7

Table 4: R^2 values data of Langmuir isotherm and Temkin isotherm

pH Values	R^2 values			
	Langmuir Isotherm	Temkin Isotherm	Florin-Huggins Isotherm	Frumkin Isotherm
2	0.763	0.945	0.691	1.000
3	0.999	0.990	0.930	0.037
4	0.953	0.998	0.763	0.011
5	0.996	0.867	0.956	0.000
6	0.964	0.867	0.604	1.000
7	0.996	0.023	0.447	0.000
Average R^2 values	0.945	0.782	0.731716667	0.3413

IV. Conclusion

The anticorrosive properties of sea mango oil were investigated on mild steel AISI 1018 specimens in test solutions consisting formulated CIT20H of different concentration at pH 2 to pH 7, using weight loss method and electrochemical method (Potentiodynamic Tafel Polarization). Besides, characterization of sea mango oil was studied using FTIR and GCMS. Based on the results obtained in the present research, the following conclusions may be drawn:

(1). Formulation of CIT20 shows that sea mango oil exhibits good dilution with distilled water and stable for the test solutions experimented.

(2). Phytochemical tests showed the presence of steroid in sea mango oil.

(3). FTIR and GCMS has proved that the presence of lone pair electrons in oxygen and nitrogen besides double and triple bonds have become the factor of good corrosion inhibiting properties.

(4). Sea mango oil portrays good inhibiting properties for mild steel in solution of pH 2 to pH 7 for both weight loss test and electrochemical test that its inhibition increases as the concentration of inhibitor increases. Besides, corrosion rate of mild steel also decreases.

(5). Sea mango oil obeyed Langmuir isotherm adsorption mechanism.

Acknowledgment

Thank you to my supervisor, Dr. Nor Roslina Rosli for endless support and guidance throughout this experimental study.

References

[1] D. K. Singh, S. Kumar, G. Udayabhanu, and R. P. John, "4(N,Ndimethylamino) benzaldehyde nicotinic hydrazone as corrosion inhibitor for mild steel in 1MHCl solution: An experimental and theoretical study," Journal of Molecular Liquids, vol. 216, pp. 738–746, 2016

[2] Obot, I.B., Umoren, S. A., Obi-Egbedi, N.O., (2011). Corrosion inhibition and adsorption behaviour for aluminuim by extract of Aningeria robusta in HCl solution: Synergistic effect of iodide ions. Journal of Materials and Environmental Science. 2 (1):60-71.

[3] M. M. Solomon and S. A. Umoren, "Enhanced corrosion inhibition effect of polypropylene glycol in the presence of iodide ions at mild steel/sulphuric acid interface," Journal of Environmental Chemical Engineering, vol. 3, no. 3, pp. 1812–1826, 2015.

[4] P. Roy, P. Karfa, U. Adhikari, and D. Sukul, "Corrosion inhibition of mild steel in acidic medium by polyacrylamide grafted Guar gum with various grafting percentage: effect of intramolecular synergism," Corrosion Science, vol. 88, pp. 246–253, 2014.

[5] Chigondo, Marko, and Fidelis Chigondo. 2016. "Recent Natural Corrosion Inhibitors for Mild Steel: An Overview." Journal of Chemistry 2016: 1–5.

[6] B.E. Rani and B.B. Basu. (2011, Jun.) "Green Inhibitors for Corrosion Protection of Metals and Alloys: An Overview." International Journal of Corrosion. [Online]. vol. 2012, Article ID 380217, 15 pages, Available: http://www.hindawi.com/journals/ijc/2012/380217/ [Jun. 16, 2014].

[7] Gomes, Elron Edgar. 2015. "Green Inhibition of Mild Steel Corrosion in CO2 Saturated Saline Solution." (May): 1–189.

[8] Karuppusamy, M et al. 2015. "Mimusops Elengi Linn Plant Extract as an Efficient Green Corrosion Inhibitor for Mild Steel in Acidic Environment." Journal of Environmental Nanotechnology 4(2): 09–15. http://www.nanoient.org/JENT/Volume4/Issue2/Mimusops-Elengi-Linn-Plant-Extract-as-an-Efficient-Green-Corrosion-Inhibitor-for-Mild-Steel-in-Acidic-Environment/393.

[9] Al-Rawashdeh N, Maayta A. Cationic surfactant as corrosion inhibitor for aluminium in acidic and basic solutions. Anti-Corrosion Methods and Materials. 2005;52(3):160-6.

[10] El-Wahab, E. A. A., A. H. Marei, O. R. Khalifa, and H. A. Mohamed. 2010. "Corrosion Behavior of Aluminum Electrode in Absence and in Presence of Sodium Chloride at Different pH Solutions Using Toludine as Inhibitor." Journal of American Science 6(8): 476–86. http://www.jofamericanscience.org/journals/am-sci/am0608/59_3379am0608_476_486.pdf.

[11] Cang, Hui et al. 2013. "Corrosion Inhibition of Mild Steel by Aloes Extract in HCl Solution Medium." 8: 720–34.